Ionic and covalent electronic states for K adsorbed on Cu5 and Cu25 cluster models of the Cu(100) surface

Paul S. Bagus and Gianfranco Pacchioni

Citation: The Journal of Chemical Physics **102**, 879 (1995); doi: 10.1063/1.469154
View online: http://dx.doi.org/10.1063/1.469154
View Table of Contents: http://scitation.aip.org/content/aip/journal/jcp/102/2?ver=pdfcov
Published by the AIP Publishing

Ionic and covalent electronic states for K adsorbed on Cu_5 and Cu_{25} cluster models of the Cu(100) surface

Paul S. Bagus
IBM Research, Almaden Research Center, 650 Harry Road, San Jose, California 95120-6099

Gianfranco Pacchioni
Dipartimento di Chimica Inorganica, Metallorganica e Analitica, Centro CNR, Universita' di Milano, via Venezian 21, 20133 Milano, Italy

(Received 20 June 1994; accepted 4 October 1994)

The chemisorption of K on the fourfold hollow site of the Cu(100) surface has been theoretically investigated by means of Cu_5–K and Cu_{25}–K cluster models. We have analyzed Hartree–Fock self-consistent field (SCF) wave functions for various electronic states of the two clusters. Four different measures have been used to establish the degree of ionicity of each state: (1) the analysis of the dipole moment curve for the variation of the Cu–K distance; (2) a constrained variation of the SCF orbitals to separate electrostatic, polarization, and charge transfer contributions; (3) the projection of the K valence orbitals onto the cluster wave function to measure the orbital occupancies, and (4) an energetic analysis of the cost and benefit of forming an ionic bond. We found different properties for the two clusters. All the considered electronic states of Cu_{25}–K show large ionic character, suggesting that the bonding of K to a Cu(100) surface is indeed ionic at low coverage. The bonding character of the lowest states of Cu_5–K is different, ranging from dominantly ionic to dominantly covalent. This behavior for Cu_5–K is related to the small size of the cluster but it can be useful for modeling the transition from ionic to metallic bonding as the coverage of the alkali metal increases. © *1995 American Institute of Physics.*

I. INTRODUCTION

The nature of the bonding of adsorbates on metal surfaces has been successfully described and analyzed by means of cluster model wave functions.[1] The determination of the electronic structure of an adsorbed atom or molecule on a cluster chosen to represent the substrate can be performed employing sophisticated quantum-mechanical electronic wave functions. Thus, it is possible to study a large number of phenomena at solid surfaces. In particular, the cluster wave functions make it possible to easily describe the adsorbate–substrate interaction and the chemisorption bond in terms of the chemical concepts that are used for molecular systems. However, there is often an uncertainty in the reliability of the chemisorption bond energy obtained with the cluster model; this uncertainty may be of the order of 1 eV, depending on the kind of bonding considered. It arises because of the limited representation of the substrate conduction band of the substrate which is given by small and modest size clusters.[2] The approach of ''bond preparation'' has been proposed by Siegbahn and collaborators, see, e.g., Ref. 3, as a way to reduce the uncertainty in the chemisorption bond energy. It is based on the use of excited states which are assumed to give a better description of the chemical bonding between the adsorbate and the substrate. This approach is an extension of an idea introduced some time ago by Hermann *et al.*;[4] however, in the early work, the excited states were used only to obtain qualitative information about the bond character when very small clusters were used. Recent results by Ricart *et al.*[5] for CO interacting with a five-atom cluster model of Cu(100), indicates that the major effect of changing the cluster state is to change the nonbonding, or Pauli, repulsion between surface and adsorbate; changes in the chemical bond were considerably smaller. Thus, the bond preparation approach could involve choosing a cluster state with a Pauli repulsion which gives a chemisorption bond energy in agreement with values determined from experimental data; in such cases, bond preparation must be viewed as an empirical procedure. Hence, it would appear to be desirable to try to obtain accurate chemisorption bond energies by using embedding schemes where the cluster wave function is determined with boundary conditions which take into account the effects of the rest of the crystal.[6–8]

Despite the uncertainty of the bond energies, other properties, such as bond distances, vibrational frequencies, and most important of all, the character of the chemisorption bond, are relatively insensitive to the choice of the cluster, the choice of the electronic state, and whether electron correlation effects are treated. Thus, the nature of adsorbate–surface bonding is in general the same for different cluster sizes, electronic states, and wave functions.

In a series of recent papers, we have analyzed the bonding of electronegative atomic and molecular adsorbates, like F, Cl, Br on Ag (111),[9,10] SCN on Ag(100),[11] and CN on Cu (100).[12] We have found that some properties depend strongly on the cluster size while others depend only weakly on the size. The binding energy, D_e, and the dipole moment at equilibrium, μ_e, change by a large amount with different cluster sizes because their values are determined, to a large extent, by the cluster representation of the surface charge distribution. On the other hand, properties that reflect the character of the bond between adsorbate and substrate change very little with different cluster sizes. For all these cases, the adsorbate bonding is dominantly ionic and the adsorbate atom or molecule becomes essentially a complete anion. Co-

valently bonded adsorbates, like CO on metal surfaces, also exhibit the same bonding mechanism for different cluster sizes, adsorption sites, and electronic states.[2,5,13,14] The study of the cluster-size dependence of the binding energy of CO on the Cu(100) surface[2] has shown a clear correlation between the positions of the cluster highest occupied molecular orbitals (HOMOs) for σ and π symmetries and the Cu–CO D_e. The oscillations in the D_e are caused by the changes in the Pauli repulsion between the CO molecule and the cluster charge distribution. The other bonding mechanisms remain more or less constant as the cluster size changes.

In this paper, we carefully analyze the nature of the Cu (100)/K bonding obtained from *ab initio* cluster wave functions. We show that this bonding changes as function of both cluster size and cluster electronic state when small clusters are considered. We will present and discuss results for two cluster models, Cu_5–K and Cu_{25}–K, of the adsorption of K on the fourfold hollow site of the Cu(100) surface. This choice is justified by the fact that alkali metal atoms are believed to occupy preferentially high-coordinated sites,[15–17] although recently examples of on-top adsorption have been reported.[18,19] On the Cu(100) surface, however, the fact that K adsorbs in fourfold hollow sites is well established.[16] All the considered states for the larger Cu_{25}–K cluster exhibit the same ionic character and can thus be described as Cu_{25}^{-}/K^{+}. In Cu_5–K, on the contrary, there are three low-lying states with completely different character: ionic, covalent, and mixed, respectively. One important reason for this behavior is that the cluster electron affinity, EA, for a very small cluster, like Cu_5, is very small and may even be negative; the EA becomes larger with increasing cluster size.[20,21] A second important reason is that a very small cluster has only a limited response to the presence of an ionic adsorbate and small clusters do not give a good representation of the surface image charge. Neither of these factors favors forming an ionic bond. However, this dependence of the bonding nature on the cluster and on a given electronic state can be used to model different situations,[20] like the evolution of the Cu/K interaction from fully ionic at low coverage to metallic (covalent) at monolayer coverage.

II. COMPUTATIONAL DETAILS

A. Cluster models of the Cu(100) surface

Two clusters, Cu_5 and Cu_{25}, shown in Fig. 1, were used to model the four-hollow adsorption site on a regular, unreconstructed, Cu(100) surface. In Cu_5 only the first nearest neighbors are represented, four in the first layer and one in the second, of an adsorbed K atom. In Cu_{25} the second neighbors in the first and second layer were added. All the Cu atoms are fixed at the positions for a bulk crystal. The distance of K from the surface, z, was varied and the properties of the Cu/K bond were studied as function of z.

The K/Cu ratio in the two clusters is very different; in Cu_{25}–K there is only 1 K atom for 16 surface Cu atoms. For this reason, the Cu_{25}–K cluster models low coverage of K on the surface. In Cu_5–K there is only 1 K for 4 surface Cu atoms. Thus, Cu_5–K can eventually model situations where the coverage, θ, is high, as shown further below.

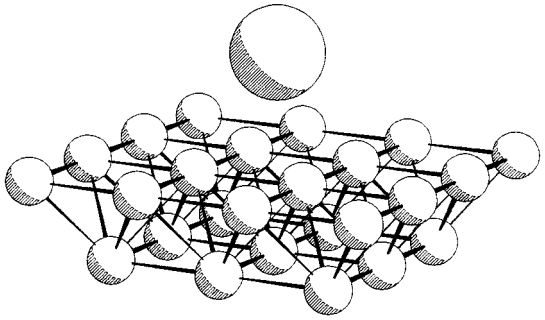

FIG. 1. Geometry of the Cu_5–K and Cu_{25}–K cluster models of Cu(100)/K. The Cu_5 and Cu_{25} clusters contain 4 and 16 atoms in the first layer and 1 and 9 atoms in the second layer, respectively. The K atom is adsorbed in a fourfold hollow position; hence, the Cu_5 cluster includes only the first neighbors of K, while second nearest neighbors in the first and second layer are present in Cu_{25}. The Cu atoms are fixed at the positions for a bulk crystal.

The focus of our cluster model studies is on the features of the interaction between the adsorbate and the substrate. In particular, the mechanisms and the trends which provides the qualitative understanding of the adsorbate–surface bond.

B. Method and cluster electronic states

Self-consistent field, SCF, Hartree–Fock wave functions were obtained by expanding the molecular orbitals in a basis of contracted Gaussian type atomic orbitals. Effective core potentials, ECPs, were used to represent the cores of the Cu atoms. For the 5 Cu atoms closest to K (all the atoms in Cu_5) the $1s^2$–$2p^6$ Ne core is replaced by a 19-electron ECP;[22] in Cu_{25}, the surrounding 20 Cu atoms are treated by means of a 1-electron ECP which includes only the valence 4s electron.[23] The 19-electron ECP atoms are described by a $[5s,5p,4d/4s,2p,2d]$ basis set;[22] the environmental 1-electron ECP Cu atoms are treated by a $[4s,4p/2s,1p]$ basis set.[23] All the electrons of the K atom were included in the wave function and a $[14s,10p/8s,6p]$ basis set was used.[24]

The lowest state of Cu_5 and Cu_{25} clusters is $^4A_2$ $(a_1)^1(e)^2$; both the e and a_1 HOMOs are of $4sp$ character. In both clusters the charge is uniformly distributed over the Cu atoms in the two layers as shown by the small dipole moments and by the similar gross atomic charges. A Cu–K covalent bond could be formed if the a_1 HOMO of Cu_5 or Cu_{25} mixes with the K 4s orbital in Cu_n–K, with direct coupling of the Cu_n $(a_1)^1$ electron with the K $(4s)^1$ electron; this results in a $^3A_2$ $(a_1)^2(e)^2$ state. In principle, it is also possible to form a covalent bond if the e HOMO of Cu_n mixes with the K 4p orbital. However, the energetic cost of promoting the K 4s electron into the 4p orbital is rather high, as shown by the energy of the respective atomic states, $E[K(^2S)]-E[K(^2P)]\simeq 1.5$ eV.[25] A Cu–K ionic bond could be formed if the K 4s electron were placed into the e orbitals of the Cu_n cluster, giving rise to the ^3E $(a_1)^1(e)^3$ configuration; however, the best candidate for a Cu–K ionic bond is the $^1A_1$ $(a_1)^0(e)^4$ configuration because here the a_1 orbital, which can mix with the K 4s, is empty.

TABLE I. SCF properties of the $^3A_2$, ^3E, and $^1A_1$ states of Cu_5K and $Cu_{25}K$. The relative energies, ΔE in eV, the equilibrium distance of K above the cluster surface, z_e in bohrs, and the vibrational frequency of K normal to the surface, ω_e in cm^{-1}, are given. The slope, M_1 in a.u./bohr, and the curvature, M_2 in a.u./$bohr^2$, of the dipole moment curve, $\mu(z)$, are given for a polynomial expansion about 6.0 bohr, see Eq. (2).

		ΔE[a]	z_e	ω_e	M_1	M_2
Cu_5K[b] $^3A_2$	$(a_1)^2(e)^2$	+0.51	6.15	89	0.28	−0.05
			(6.58)	(61)	(−0.03)	(−0.10)
Cu_5K ^3E	$(a_1)^1(e)^3$	0.00	5.94	95	0.60	0.09
Cu_5K $^1A_1$	$(a_1)^0(e)^4$	+0.37	5.79	101	0.98	0.06
$Cu_{25}K$ $^3A_2$	$(a_1)^2(e)^2$	0.00	5.95	108	0.90	0.08
$Cu_{25}K$ ^3E	$(a_1)^1(e)^3$	+0.24	5.86	110	0.90	0.08
$Cu_{25}K$ $^1A_1$	$(a_1)^0(e)^4$	+0.56	5.79	112	0.91	0.08

[a]With respect to the lowest configuration.
[b]The CASSCF results are given in parentheses.

All these states have been considered for both Cu_5–K and Cu_{25}–K and, of course, the actual nature of the interaction is determined by the variational SCF wave function for each state. All three states are close in energy and lie within 0.5 eV of each other, Table I, but their nature may be quite different, as will be discussed below.

For Cu_5–K, correlation effects were included by performing complete active space, CASSCF, calculations. The CASSCF wave functions were obtained for the lowest, $^3A_2$, state of Cu_5–K by redistributing two electrons between the Cu_5 a_1 HOMO and the K $4s$ orbital; clearly, this is a very limited configuration interaction (CI) calculation which does not include dynamical correlation effects. The reason for considering this CASSCF wave function is that, differently from the SCF one, it allows the correct dissociation of the system into neutral Cu_5 and K fragments. Since, as will be shown below, the Cu_5–K bond for the $^3A_2$ state is covalent, the CASSCF wave function gives a better representation of the D_e and of other properties, e.g., the dipole moment curve.

III. ANALYSIS OF *AB INITIO* WAVE FUNCTIONS

The relative energies, ΔE, equilibrium distances of K from the Cu_n cluster first layer, z_e, and the harmonic approximation vibrational frequencies, ω_e, for the various states considered are given in Table I. In Cu_5–K the three states have slightly different equilibrium distances, from $\simeq$5.8 to $\simeq$6.2 bohr; the potential energy curves are very flat for all three states and the corresponding vibrational frequencies are low and similar, 90–100 cm^{-1}. The CASSCF curve for the $^3A_2$ state is even more flat, ω_e=61 cm^{-1}. When potential energy curves are very flat, as in the present case, small changes in the curve can lead to large changes in the bond distance, z_e; thus, it is not particularly significant that the CASSCF value for z_e is $\simeq$0.4 bohr or 7% larger than the SCF value, Table I. In Cu_{25}–K, $z_e\simeq$5.9 and $\omega_e\simeq$110 cm^{-1} are nearly the same for the three states. From these data it is not easy to get information about the different character of the electronic states. This can be deduced, however, from other measurements and observables which provide more indirect evidence about the nature of the states. These are: (a) the analysis of the dipole moment curve as function of z (K);[9,10] (b) a constrained space orbital variation, CSOV,[26,27] which allows one to decompose the interaction energy and the dipole moment into the sum of various contributions; (c) the expectation value of a projector operator which measures the orbitals occupancies;[11] and (d) a cost/benefit analysis of the energetics of the bond formation. None of these techniques alone necessarily provide compelling evidence for the character of the bond: however, when all the measures indicate the same bond character, the nature of the interaction is definitively established.

A. Dipole moment curves

It is generally believed that the change in the value of the dipole moment in the direction of the surface normal, μ_z, or, more precisely, in the value of the work function, Φ, from the clean to the covered surface provides a measure of the ionicity of the adsorbate. Alkali metal adsorption at low coverage leads to a rapid decrease of the work function, then, at a critical coverage, the curve shows a minimum with a subsequent rise towards the value characteristic of the metallic overlayer.[28] However, the absolute value of the change in Φ, $\Delta\Phi$, is largely determined by the polarization of the substrate and does not reflect the real extent of the charge asymmetry between surface and adsorbate.[29] A better measure is given by the shape and slope of the dipole moment curve as function of the position of the adsorbate above the surface, $\mu_z(z)$, where z is taken as the direction of the surface normal. The dipole moment, μ, of a set of electronic and nuclear charges is

$$\mu=\Sigma_A Z_A R_A+\Sigma_i r_i\,, \tag{1}$$

where R (r) are the nuclear (electronic) coordinates and Z_A is the nuclear charge. Consider an expansion of the component of the dipole moment curve normal to the surface, $\mu_z(z)$

$$\mu_z(z)=M_0+M_1(z-z_e)+M_2(z-z_e)^2+\cdots, \tag{2}$$

where $M_1=d\mu/dr$, $M_2=d^2\mu/dr^2$, and $M_0=\mu_z$ for $z=z_e$. The expansion is made about the equilibrium distance of the adsorbate above the surface, z_e. For an ionic bond, the dipole moment curve is almost linear and the slope is large, $|M_1|\gg|M_2|$; for an ideal ionic adsorbate with charge +1 and in absence of any polarization, in particular of the substrate, $M_1=1$ and $M_2=0$.[9,10]

From the values given in Table I it is clear that all the states of Cu_{25}–K have a large slope, $M_1\simeq$0.9 a.u./bohr, and a small curvature, indicating that the bonding is strongly ionic for all three states; on the other hand, the three Cu_5–K states do exhibit different character. The $^1A_1$ state has a very similar $\mu_z(z)$ slope, M_1=0.98, as the Cu_{25}–K states, and can thus be classified as a largely ionic state. The slope of the $^3A_2$ state, on the contrary, M_1=0.28, is very small, and typical of covalent interactions. The CASSCF dipole moment curve shows an even smaller slope and a larger curvature, Table I; this provides an indication of an increased covalent character of the $^3A_2$ state of Cu_5–K in the correlated wave function. Thus, the dipole moment curves indicate a different character of the $^3A_2$ states in Cu_5–K and Cu_{25}–K. The Cu_5–K ^3E state has a slope, M_1=0.60, which is intermediate between the

TABLE II. CSOV analysis of interaction energy, E_{int} in eV, and dipole moment, μ in a.u., for three states of Cu_5K [for $z(K)=5.75$ bohr] and $Cu_{25}K$ [for $z(K)=5.70$ bohr].

		$E_{int}/\Delta E_{int}$		$\mu/\Delta\mu$	
State	Step[a]	Cu_5K	$Cu_{25}K$	Cu_5K	$Cu_{25}K$
$^3A_2$	FO	2.54/⋯	2.39/⋯	8.32/⋯	7.63/⋯
	V(Cu,Cu)	2.75/+0.21	3.52/+1.13	7.01/−1.31	3.41/−4.22
	V(Cu,all)	4.43/+1.68	3.74/+0.22	2.50/−4.51	3.44/+0.03
	Full SCF	4.45/+0.02	3.76/+0.02	2.46/−0.04	3.42/−0.02
^3E	FO	2.87/⋯	2.53/⋯	6.55/⋯	8.29/⋯
	V(Cu,Cu)	3.06/+0.19	3.69/+1.16	5.69/−0.86	3.94/−4.35
	V(Cu,all)	3.78/+0.72	3.88/+0.19	3.19/−2.50	4.00/+0.06
	Full SCF	3.79/+0.01	3.90/+0.02	3.16/−0.03	3.98/−0.02
$^1A_1$	FO	3.10/⋯	2.64/⋯	4.65/⋯	8.99/⋯
	V(Cu,Cu)	3.33/+0.23	3.82/+1.18	3.78/−0.87	4.45/−4.54
	V(Cu,all)	3.61/+0.28	4.00/+0.18	2.80/−0.98	4.57/+0.12
	Full SCF	3.62/+0.01	4.01/+0.01	2.78/−0.02	4.55/−0.02

[a]See the text for definition.

"covalent" $^3A_2$ and the "ionic" $^1A_1$ states; thus, on this basis, its nature should be classified as "mixed."

B. Constrained space orbital variation

The relative importance of electrostatic, polarization, and covalent bonding effects in the Cu–K interaction can be evaluated by determining the SCF wave function with some constraints.[26,27] Values of the interaction energy, E_{int}, at each CSOV step determined for $z \simeq z_e$ for all states of Cu_5–K and Cu_{25}–K are given in Table II. Potential energy curves, $V(z)$, given by the CSOV and full SCF wave functions for the $^3A_2$ states of Cu_5–K and Cu_{25}–K are shown in Figs. 2 and 3.

The starting point of the analysis is the frozen orbital, FO, interaction of Cu_n^- ($^3A_2$, ^3E, or $^1A_1$) and $K^+(^1S)$. Here, the SCF charge densities determined for the isolated Cu_n^- and K^+ ions are kept fixed. The only interactions possible for the FO starting point are the Coulomb attraction of the ions and the Pauli repulsion arising from the overlap of the two charge distributions. The electrostatic attraction for $z \simeq 5.7$ bohr is large, 2.5–3 eV, for all states, see Table II. The minimum of the $V(z)$ curve at the FO step is at z(Cu–K)≃7 bohr for both Cu_5–K and Cu_{25}–K, see Figs. 2 and 3. For z(K) <6.5 bohr, the FO potential energy curves begin to rise rapidly since the interpenetration of the Cu_n^- and K^+ charge distributions increases exponentially.

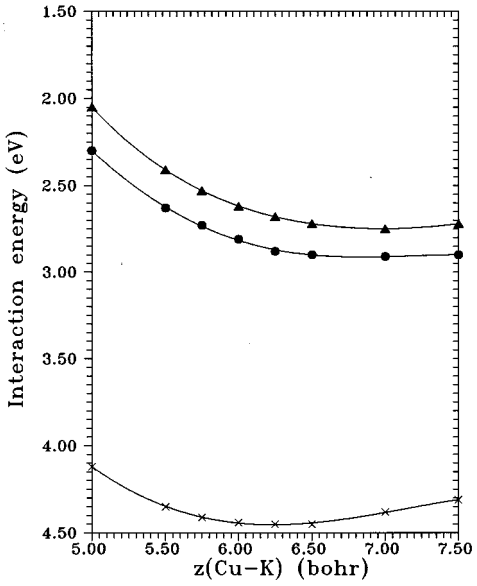

FIG. 2. Potential energy curves for Cu_5–K ($^3A_2$) as function of the height of the K atom from the cluster surface. The zero of energy for the frozen orbital (▲), Cu Polarization (●), and full SCF (×) curves is E_{SCF} [Cu_5^- ($^3A_2$)]+E_{SCF}[$K^+(^1S)$].

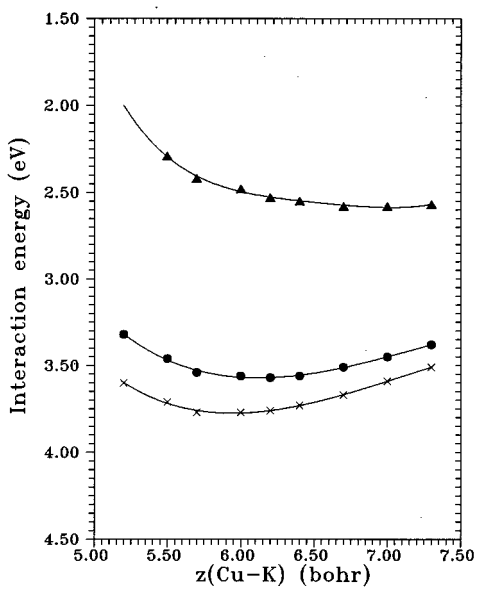

FIG. 3. Potential energy curves for Cu_{25}–K ($^3A_2$) as function of the height of the K atom from the cluster surface. The zero of energy for the frozen orbital (▲), Cu Polarization (●), and full SCF (×) curves is E_{SCF}[$Cu_{25}^-(^3A_2)$]+E_{SCF}[$K^+(^1S)$].

In the next step, V(Cu,Cu), the orbitals of the Cu cluster are allowed to vary in the Cu space only and the K^+ orbitals are fixed at their atomic character. In particular, charge transfer or covalent bonding between Cu and K is not allowed at this step because the unoccupied K^+ $4s$ and $4p$ orbitals, as well as other K^+ virtual orbitals, are explicitly excluded from the variational space. At this step, the Cu_n^- electrons polarize in response to the presence of the K^+ cation. The attraction of K^+ moves the center of the Cu charge toward the cation. Charge density difference maps, defined as the difference between the charge density obtained at the Cu polarization and at the FO step clearly show that the Cu substrate electrons move toward the K ion to screen the positive charge.[30] The response of the two clusters, Cu_5 and Cu_{25}, however, is very different. In Cu_5 the contribution from the metal polarization is small, $\simeq$0.2 eV, for all states, Table II. Clearly, this small cluster has too few atoms and electrons to provide a good representation of the highly polarizable Cu $4sp$ conduction band. In Cu_{25}–K, on the contrary, the Cu polarization contribution is large, $\simeq$1.2 eV, and again is nearly the same for the three states, see Table II.

Once the Cu polarization is taken into account in the Cu_{25}–K $^3A_2$ state, z_e=6.1 bohr and ω_e=102 cm^{-1} are reasonably close to the unconstrained, full SCF values, z_e=5.95 bohr and ω_e=108 cm^{-1}, see also Fig. 3. For the Cu_5–K $^3A_2$ state, after inclusion of the Cu_5 polarization, z_e=6.9 bohr and ω_e=73 cm^{-1} are very different from the corresponding full SCF values, z_e=6.15 bohr and ω_e=89 cm^{-1}, see also Fig. 2. This suggests that in Cu_{25}–K the most important bonding contributions are the electrostatic interaction between Cu_{25}^- and K^+ and the Cu polarization, while in Cu_5–K there must be other terms which have not yet been included in the wave function.

In the next CSOV step, V(Cu,all), the occupied Cu orbitals are allowed to mix with the virtual K^+ orbitals. This corresponds to the formation of a dative covalent bonding and the energetic importance of this interaction is measured by the $\Delta E_{\rm int}$ value at the V(Cu,all) step, see Table II. In Cu_{25}–K this contribution is small, $\simeq$0.2 eV, only $\simeq$5% of the total interaction energy between Cu_{25}^- and K^+. The same is true for the ionic $^1A_1$ state of Cu_5–K where $\Delta E_{\rm int}$ at the V(Cu,all) step is $\simeq$0.3 eV. In the ^3E and $^3A_2$ states of Cu_5–K, however, the covalent bonding lowers the interaction energy by 0.7 and 1.7 eV, respectively, indicating the occurrence of a considerable covalent bonding of the Cu_n^- conduction band levels and the K^+ $4s$ and $4p$ levels. This is consistent with the description of the two states as mixed and covalent, respectively. Once the covalent mixing is allowed, z_e=6.17 bohr and ω_e=88 cm^{-1} at the V(Cu,all) step are very close to the final, full SCF, values for the $^3A_2$ state of Cu_5–K, see Fig. 2. The large energy lowering at the V(Cu,all) step for the ^3E and $^3A_2$ states of Cu_5–K is a real effect and does not arise from the poor description of the Cu_5^- $^3A_2$ state with the basis set used. This is shown by the small basis set superposition error, BSSE, which for Cu_5^- is only 0.09 eV. The energy decrease at the V(Cu,all) step is 1.7 eV and therefore the BSSE is responsible only for 5% of this stabilization, the rest being due to the formation of a covalent bond. Even smaller BSSEs, $<$0.03 eV, are found for K^+ or for neutral Cu_5 ($^4A_2$) and K (^2S).

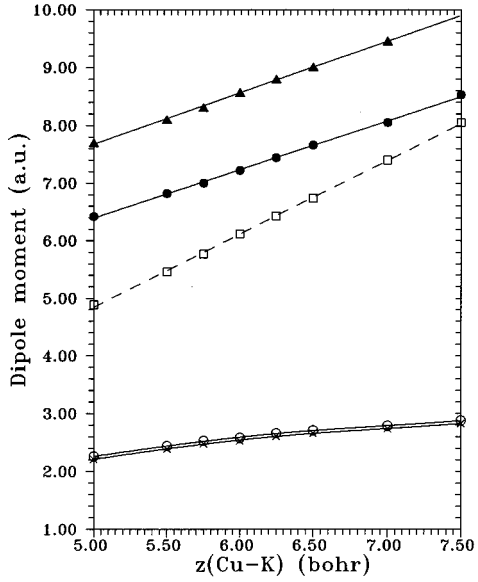

FIG. 4. Dipole moment curves for Cu_5–K ($^3A_2$). Curves are given for the frozen orbital (▲), Cu polarization (●), Cu donation (○), and full SCF (×) wave functions (see the text). The curve for Cu_5^-($^3A_2$) interacting with a point charge of +1 is also shown (□). μ in a.u., 1 a.u.=2.54 D.

The CSOV decomposition can be performed also for the dipole moment curve, $\mu(z)$. In Figs. 4 and 5 are shown the dipole moment curves for the frozen orbital (FO), Cu polarization [V(Cu,Cu)], Cu donation [V(Cu,all], and full SCF wave functions for the $^3A_2$ states of Cu_5–K and Cu_{25}–K. The corresponding M_0, M_1, and M_2 values, see Eq. (2), are

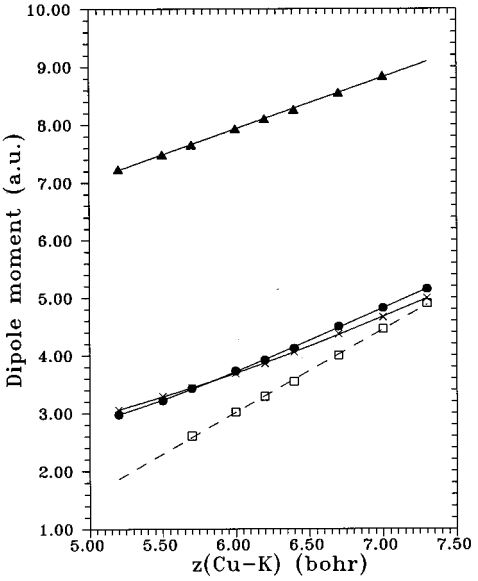

FIG. 5. Dipole moment curves for Cu_{25}–K ($^3A_2$). Curves are given for the frozen orbital (▲), Cu polarization (●), and full SCF (×) wave functions (see the text). The curve for Cu_{25}^- ($^3A_2$) interacting with a point charge of +1 is also shown (□). μ in a.u., 1 a.u.=2.54 D.

TABLE III. Dipole moment, M_0 in a.u., slope, M_1 in a.u./bohr, and curvature, M_2 in a.u./bohr^2, of the dipole moment curves, $\mu(z)$, determined at various CSOV steps for a polynomial expansion about 6.0 bohr, see Eq. (2).

		FO	V(Cu,Cu)	V(Cu,all)	Full SCF
Cu_5–K $^3A_2$	M_0	8.55	7.21	2.57	2.53
	M_1	0.90	0.82	0.28	0.28
	M_2	0.01	0.01	−0.06	−0.05
Cu_5–K ^3E	M_0	6.79	5.92	3.34	3.32
	M_1	0.93	0.91	0.60	0.60
	M_2	0.02	0.04	−0.09	−0.09
Cu_5–K $^1A_1$	M_0	4.89	4.03	3.04	3.02
	M_1	0.95	1.02	0.98	0.98
	M_2	0.02	0.04	0.06	0.06
Cu_{25}–K $^3A_2$	M_0	7.92	3.72	⋯	3.69
	M_1	0.88	1.02	⋯	0.90
	M_2	0.03	0.10	⋯	0.08

given in Table III also for the other Cu_5–K states. The $\mu(z)$ curves computed at the different CSOV steps are compared with those of the Cu_5^- and Cu_{25}^- clusters interacting with a point charge, PC, of +1 moved along the z direction, Cu_n^-/PC.

For both systems, Cu_5–K and Cu_{25}–K, the curves for the FO wave functions are linear and the value of $\mu(z)$ near equilibrium is large and positive, as expected for a cation above the unpolarized Cu surface, see Figs. 4 and 5 and Table III; the slopes of the FO curves, ≃0.90, Table III, are smaller than 1 because of the interpenetration of the K^+ and Cu_n^- charges. The value of the dipole moment at z_e, μ, after the polarization of the Cu cluster is allowed, V(Cu,Cu), is smaller than for the FO wave function, see Table III; there is a reduction of ≃1.3 a.u. in Cu_5–K ($^3A_2$) and of more than 4 a.u. in Cu_{25}–K ($^3A_2$). This reduction follows because the Cu charge polarizes toward K^+. At the V(Cu,Cu) step the slope is M_1=0.82 for Cu_5–K and M_1=1.02 for Cu_{25}–K. Hence, the Cu polarization $\mu(z)$ curve is almost equal to the full SCF one in Cu_{25}–K, Fig. 5. However, this is not the case for Cu_5–K, Fig. 4. The different amount of covalent bonding in the two clusters can be clearly seen from the change in the slope of the $\mu(z)$ curve at the Cu donation step, V(Cu,all). While the Cu_{25}–K curve is barely affected by the inclusion of this covalent contribution, a large decrease in the slope, from M_1≃0.8 to M_1≃0.3, and in the absolute value of the dipole moment, from M_1≃7.2 a.u. to M_1≃2.6 a.u., is found at this step for the Cu_5–K $^3A_2$ state, see Fig. 4 and Table III. This effect is less pronounced for the ^3E and almost negligible for the $^1A_1$ Cu_5–K states, respectively, see Table III.

It is interesting to compare the values of the $\mu(z)$ curves with those of the Cu_n^-/PC clusters. The shape for the Cu_{25}^-/PC cluster $\mu(z)$ curve is similar to those for the Cu_{25}–K Cu polarization and full SCF wave functions, see Fig. 5. This is further evidence that the Cu_{25}–K $^3A_2$ state is, indeed, ionic. The slope of the $\mu(z)$ curve for Cu_{25}^-/PC, M_1=1.37, is somewhat larger than the slope of the SCF curve for Cu_{25}–K, M_1=0.90, mainly because the polarization is different when Cu responds to a point charge and to an extended K^+ ion.[30] The $\mu(z)$ curve for Cu_5^-/PC, on the contrary, shows a completely different behavior from that of the full SCF Cu_5–K $^3A_2$ wave function, see Fig. 4. This is not surprising given the completely different character of an adsorbed neutral K atom and of a PC.

TABLE IV. Changes, ΔP, in the expectation value of the projection, $P(\phi)$, of K 4s and 4p orbitals on $\Psi(Cu_nK)$ at various CSOV steps measuring the change in occupation of the K 4s and 4p orbitals.

	Cu_5K ($^3A_2$)		$Cu_{25}K$ ($^3A_2$)	
Step B−Step A[a]	$\Delta P(4s)$	$\Delta P(4p)$	$\Delta P(4s)$	$\Delta P(4p)$
V(Cu,Cu)-frozen orbital	0.05	−0.02	0.12	0.24
V(Cu,all)−V(Cu,Cu)	0.48	−0.15	0.02	−0.05

[a]See the text for definition.

C. Occupation of K 4*sp* orbitals

Another method to characterize ionicity makes use of an orbital projection operator.[10] The projection of an orbital, $P(\phi)$, is the expectation value of the operator $\phi\phi^+$ over the wave function of the system, Ψ,

$$P(\phi)=\langle\Psi|\phi\phi^+|\Psi\rangle, \tag{3}$$

and it measures the extent to which the orbital ϕ is contained in the total wave function for the adsorbate–substrate system. In the special case that $P(\phi)$≃1 or 0 for spin orbital ϕ, the interpretation is clear; the orbital ϕ is either fully occupied or empty in the cluster. Much less transparent is the interpretation of the values of $P(\phi)$ when they are not integer, as in covalent interactions. For the case where the value of P is fractional, corrections must be made to take into account the overlap of the adsorbate orbitals with the orbitals of the bare substrate cluster.[10,12]

For the 4s and 4p orbitals of K, we use projection operators for the 4s and for the sum of the three degenerate 4p orbitals. The orbitals used to form the projection operator are the SCF 4s orbitals for the ground, ^2S, and the 4p orbital for the first excited, ^2P, state of neutral K. The K 4s and 4p character have been projected from the wave function for each of the CSOV steps for the $^3A_2$ states of the Cu_5–K and Cu_{25}–K clusters. We take the overlap of the adsorbate and substrate orbitals into account by considering the differences of the projection, $\Delta P(4s)$ and $\Delta P(4p)$, between consecutive CSOV steps rather than the absolute value of P for any particular step. At the FO step, there is by construction no 4s or 4p character, and the ΔP for the following CSOV steps indicate the changes in the apparent 4s and 4p character along with the chemical reasons for the changes. In Table IV, we report the changes in the projection, $\Delta P(4s)$ and $\Delta P(4p)$, for two cases: (a) between the V(Cu,Cu) and the FO steps; these ΔP reflect the cluster polarization. (b) Between the V(Cu,all) and the V(Cu,Cu) wave functions; these ΔP actually measure the extent of charge transfer from Cu to K. The effect of the Cu polarization on the projection is negligible for Cu_5–K, Table IV; this is expected, given the low energy lowering and dipole moment change associated with this mechanism. In Cu_{25}–K the $\Delta P(4s)$ and $\Delta P(4p)$ due to the Cu polarization are larger, Table IV; this is an additional proof of the important charge redistribution occurring when the Cu electrons are free to respond to the presence of the

TABLE V. Cost/benefit analysis for the formation of a covalent or an ionic Cu–K bond. The E_{int}(ions) value, in eV, is the sum of the electrostatic attraction between Cu_n^- and K^+ plus the polarization of the Cu_n substrate; see V(Cu,Cu) CSOV step in Table II. The values are for SCF wave functions for z(K)=5.75 bohr (Cu_5K) and z(K)=5.70 bohr (Cu_{25}K).

		E_{int}(ions) (eV)	IP(K)[a] (eV)	EA(Cu_n)[b] (eV)	E_{cost}= IP-EA	Balance	Character
Cu_5K	$^3A_2$	+2.75	+4.01	−0.53	+4.53	$E_{int}<E_{cost}$	Covalent
	^3E	+3.06	+4.01	+1.09	+2.92	$E_{int}\simeq E_{cost}$	Mixed
	$^1A_1$	+3.33	+4.01	+0.90	+3.11	$E_{int}>E_{cost}$	Ionic
Cu_{25}K	$^3A_2$	+3.52	+4.01	+1.17	+2.84	$E_{int}>E_{cost}$	Ionic
	^3E	+3.69	+4.01	+0.71	+3.30	$E_{int}>E_{cost}$	Ionic
	$^1A_1$	+3.82	+4.01	+2.19	+1.82	$E_{int}>E_{cost}$	Ionic
Cu(100)	expt.	⋯	+4.34	+4.59	−0.25		

[a]IP(K)=$E(K^+)-E(K)$.
[b]EA(Cu_n)=$E(Cu_n)-E(Cu_n^-)$.

ionic adsorbate. In effect, the polarized Cu conduction band electrons at the V(Cu;Cu) CSOV step occupy a portion of the space which the K 4s and 4p orbitals would occupy if they were present. This is clearly seen in the density difference plots given in Ref. 30. The polarized Cu conduction band charge occupies only a region between the K^+ ion and the Cu cluster. It does not extend to the other side of the K^+ ion as would happen if the K 4s or 4p orbitals were occupied.

At the V(Cu,all) step, where charge transfer from Cu_n^- to K^+ is allowed, there is a large increase in the occupation of the K 4s orbital in Cu_5–K; a covalent bond is formed and electrons are shared between the two fragments. In Cu_{25}–K, on the other hand, there is no significant change in the occupation of the 4s and 4p K orbitals when covalent bonding is allowed, see Table IV.

D. Cost/benefit analysis

In this paragraph we discuss the energy balance which leads to the formation of a covalent or of an ionic bond for the different states of a cluster. A similar analysis has been reported for the Cu_{25}–K cluster;[30] here we extend the previous analysis to the case of Cu_5–K and we show that the different nature of the Cu–K bonding in the two clusters is largely determined by two cluster properties for the various electronic states considered. One property is the cluster electron affinity, EA, which in the energy balance is a part of the cost term to form the ionic units, Cu_n^- and K^+. The second property is the cluster polarizability; this polarizability contributes to the energetic benefit because it allows the Cu_n^- cluster to respond to the presence of the K^+ cation.

The energetic cost, E_{cost}, of forming the ions is given by the difference of the ionization potential, IP, of the K atom and the electron affinity, EA, for the appropriate state of Cu_n. The IP=$E(K^+)-E(K)$ is always a positive quantity; the EA=$E(Cu_n)-E(Cu_n^-)$ is defined in such a way that a positive value corresponds to the Cu_n^- cluster having a lower energy than the separated species Cu_n+e^-. While the IP can be computed with reasonable accuracy with a SCF wave function, the determination of the EA is much more complex and requires the introduction of correlation effects.[31] Thus, the EA values computed for the different states of Cu_5 and Cu_{25} clusters are much smaller in absolute value than the true EA of the metal. This is well documented by a comparison of the computed IP and EA values, see Table V, with the corresponding experimental IP of K, 4.34 eV,[25] and the Cu(100) work function, Φ=4.59 eV,[32] which is a measure of the EA of the extended metal.

The other important energetic aspect of the formation of an ionic bond is the interaction energy between K^+ and Cu_n^- at the Cu polarization step of the CSOV analysis. At this step, the total energy of the system is the sum of the electrostatic attraction between the ions and the polarization of the metal substrate. However, contributions from the dative covalent bonding between the Cu_n^- cluster orbitals and the unoccupied K 4s and 4p orbitals are not allowed at the V(Cu;Cu) CSOV polarization step. Thus, the interaction energy at this step is a proper measure of the energetic benefit of forming an ionic bond. Of course, we should take E_{int} with respect to the energy of the ionic limits and we denote this as E_{int} (ions),

$$E_{int}(\text{ions})=[E(Cu_n^-)+E(K^+)] - E[Cu_n\text{–K};\ \ V(Cu;Cu)];$$

E_{int}(ions)>0 indicates a bound system. If this E_{int}(ions) is less than E_{cost}, the price paid to form the ions, the interaction could become covalent in the full SCF wave function if a level is available for covalent bonding. If E_{int}(ions) at the Cu polarization step is already greater than E_{cost}, the ionic interaction is energetically favored. If E_{int}(ions) is about equal to E_{cost}, a state with mixed covalent and ionic character is likely. Values of E_{int}(ions) are given in Table V.

This is exactly what is found for the various Cu_5–K and Cu_{25}–K states. The addition of one electron to the $^4A_2$ state of Cu_5, open shells $a_1{}^1e^2$, to form the $a_1{}^2e^2$ $^3A_2$ state of Cu_5^- is an unfavorable process with a negative EA, Table V. Hence, the cost of forming the two ionic fragments, Cu_5^- and K^+, ≃4.5 eV, Table V, largely exceeds the energy gain which derives from the sum of the electrostatic interaction plus the metal polarization; the bonding becomes covalent when the mixing between the occupied Cu_5^- and the virtual K^+ orbitals is permitted. In the Cu_5–K ^3E state, E_{cost} is similar to E_{int}, and the resulting unconstrained wave function has a mixed

ionic–covalent character. For all the other states the formation of an ionic bond compensates for the price paid to form the ions, Table V, and the bonding remains ionic.

In this cost/benefit analysis, we have followed the original ideas due to Langmuir and Kingdom.[33] However, because we have cluster wave functions available, we are able to apply the analysis to different electronic states and to different size clusters. The covalent interaction for the Cu_5–K $^3A_2$ state follows from the large cost (Cu_5 has a negative EA), and the small benefit, (Cu_5 has a small polarization). The opposite arguments apply to the Cu_{25} electronic states. A real metal surface will be more polarizable than the Cu_{25} cluster, and the benefit obtained with this cluster is likely to be a lower limit to the benefit on Cu(100). In addition, the experimental cost of forming the ions, $E_{\text{cost}}(\text{expt})=\text{IP(K)}-\Phi[\text{Cu(100)}]=4.34-4.59=-0.25$ eV, is negative, indicating that the electron transfer from K to Cu (100) is energetically favorable for the separated real systems.

IV. DISCUSSION AND CONCLUSIONS

We have investigated the character of the Cu(100)/K bond with the help of two cluster models, Cu_5–K and Cu_{25}–K. Various electronic states have been considered, all exhibiting similar equilibrium bond distances, vibrational frequencies, and dissociation energies. The nature of each cluster electronic state has been analyzed by means of several measures which have made it possible to unambiguously identify the extent of ionicity of each state. Three of these measures are based on the analysis of SCF wave functions and related properties: (i) the dipole moment curve for the motion of the K adsorbate above the surface; (ii) the decomposition of the interaction energy and dipole moment into the sum of contributions arising from the electrostatic interaction between the ions, the polarization of the metal substrate, and the covalent bonding; (iii) the expectation value of a projection operator which measures the occupancy of the K valence orbitals. All these measures together indicate a large ionicity for the three low-lying electronic states of the Cu_{25}–K cluster, which models K chemisorption in the hollow site of the Cu (100) surface at very low coverage. On the other hand, the three low-lying states of the Cu_5–K, exhibit different characters: one state is largely ionic and closely resembles the Cu_{25}–K states; one state is largely covalent with little charge transfer; one state has a nature which is intermediate between these two extremes.

The reason for the appearance of states with completely different bonding character for the small Cu_5 cluster can be easily rationalized by considering the balance between the energetic price required to form the Cu_5^- and K^+ ionic fragments, i.e., the IP of K minus the EA of Cu_n, and the energy gain due to the formation of the ionic surface complex. This cost/benefit analysis clearly shows that the reason for the existence of electronic states with completely different character in Cu_5–K must be attributed to two factors. First, the EAs of the various Cu_5^- anion states are small and this leads to a larger energetic cost to form the cation and anion needed for an ionic bond. Second, the small Cu_5^- cluster has only a very limited polarizability and does not change substantially in the presence of K^+. Thus, the energetic benefit for Cu_5 of forming the ionic bond is largely confined to the electrostatic interaction between Cu_5^- and K^+ with only a small contribution from the Cu_5^- polarization. Clearly, the Cu_5 cluster is too small to properly describe the energetics of the interaction of K with a Cu surface for low K coverage. However, the fact that there are states of Cu_5–K with bonding ranging from dominantly ionic to dominantly covalent is very useful. These states have been used[20] to model and interpret the transition from ionic bonding at low K coverage to covalent bonding at higher K coverages.

On the other hand, the larger Cu_{25}–K cluster gives a better representation of both the EA and the polarization of the Cu(100) metal surface; for this system the benefit of forming an ionic bond exceeds the cost of forming the ions for all the states considered. Even the Cu_{25} cluster, however, provides a limited representation of the real surface which has a much larger EA and presumably a larger polarizability. Thus, the energy gain obtained with the Cu_{25} cluster is a lower limit to the real benefit of forming an ionic Cu(100)/K bond.

These results clearly show that the use of small clusters may be critical for the description of cationic species at metal surfaces. In this respect, the situation is quite different from the case where the charge transfer occurs from the cluster to the adsorbate, as for halogens on Ag.[9,10] Here, in fact, the critical quantities in the cost/benefit balance are the halogen EA and the cluster IP. The adsorbate EA can be reproduced with sufficient accuracy by including in the basis set diffuse functions. Furthermore, the cluster IP, even for small clusters, is usually rather close to the metal work function while the cluster EA converges only very slowly with increasing cluster size to the work function. Thus, while the ionic nature of the metal–halogens interaction is correctly described with small substrate clusters, relatively large clusters are needed to obtain a qualitatively correct physical picture of the adsorbate–substrate charge transfer for alkali atoms on metals.

Finally, it is worth mentioning that the determination of the character of the bonding based on an observable property like the metal–adsorbate distance is not straightforward. In low-energy electron diffraction, surface-extended x-ray absorption fine structure, and surface x-ray diffraction experiments,[15–19] the effective radius of the alkali metal has been used as a guide to distinguish between ionically or covalently bonded systems; the ionic radius of K^+, 1.33 Å, is in fact $\simeq$1 Å shorter than the covalent one, 2.38 Å. The small change in z_e for the three states of Cu_5–K, Table I, corresponding to effective K radii ranging from 2.45 Å ($^3A_2$) to 2.28 Å ($^1A_1$) does not reflect the dramatic change in the character of the bonding. Thus, no change or very small changes are expected in the Cu–K distance as the bond character evolves from ionic to covalent by increasing the coverage. This is exactly what has been observed for K on Cu(100) where an absorption height independent of the coverage has been measured by Meyerheim *et al.*[16] We have shown[20] that other properties, like the adsorbate core level shifts and the intensity of the vibrational absorption, provide a much more reliable way to determine the nature of the surface chemical bond.

[1] *Cluster Models for Surface and Bulk Phenomena*, NATO ASI Series Vol. 283, edited by G. Pacchioni, P. S. Bagus, and F. Parmigiani (Plenum, New York, 1992).
[2] K. Hermann, P. S. Bagus, and C. J. Nelin, Phys. Rev. B **35**, 9467 (1987).
[3] I. Panas, J. Schüle, P. E. M. Siegbahn, and U. Wahlgren, Chem. Phys. Lett. **149**, 265 (1988).
[4] K. Hermann, P. S. Bagus, C. R. Brundle, and D. Menzel, Phys. Rev. B **24**, 7025 (1981).
[5] J. M. Ricart, J. Rubio, F. Illas, and P. S. Bagus, Surf. Sci. **304**, 335 (1994).
[6] P. V. Madhavan and J. Whitten, J. Chem. Phys. **77**, 2673 (1982).
[7] J. Whitten, in Ref. 1, p. 375.
[8] C. Pisani, R. Dovesi, R. Nada, and L. N. Kantorovich, J. Chem. Phys. **92**, 7448 (1990).
[9] P. S. Bagus, G. Pacchioni, and M. R. Philpott, J. Chem. Phys. **90**, 4287 (1989).
[10] G. Pacchioni, P. S. Bagus, M. R. Philpott, and C. J. Nelin, Int. J. Quantum Chem. **38**, 675 (1990).
[11] G. Pacchioni, F. Illas, M. R. Philpott, and P. S. Bagus, J. Chem. Phys. **95**, 4678 (1991).
[12] C. J. Nelin, P. S. Bagus, and M. R. Philpott, J. Chem. Phys. **87**, 2482 (1987).
[13] P. S. Bagus, C. J. Nelin, W. Muller, M. R. Philpott, and H. Seki, Phys. Rev. Lett. **58**, 559 (1987).
[14] G. Pacchioni and P. S. Bagus, J. Chem. Phys. **93**, 1209 (1990).
[15] M. Van Hove, S. Y. Tong, and N. Stoner, Surf. Sci. **54**, 259 (1976).
[16] H. L. Meyerheim, J. Wever, V. Jahns, W. Moritz, P. J. Eng, and I. K. Robinson, Surf. Sci. **304**, 267 (1994).
[17] C. T. Campbell, Annu. Rev. Phys. Chem. **41**, 775 (1990).
[18] D. Fischer, S. Chandavarkar, I. R. Collins, R. D. Diehl, P. Kaukasoina, and M. Lindroos, Phys. Rev. Lett. **68**, 2786 (1992).
[19] M. Kerkar, D. Fisher, D. P. Woodruff, R. G. Jones, R. D. Diehl, and B. Cowie, Phys. Rev. Lett. **68**, 3204 (1992).
[20] G. Pacchioni and P. S. Bagus, Surf. Sci. **286**, 317 (1993).
[21] H. Akeby, I. Panas, L. G. M. Pettersson, P. Siegbahn, and U. Wahlgren, J. Phys. Chem. **94**, 5471 (1990).
[22] P. J. Hay and W. R. Wadt, J. Chem. Phys. **82**, 299 (1985).
[23] P. S. Bagus, C. W. Bauschlicher, C. J. Nelin, B. C. Laskowski, and M. Seel, J. Chem. Phys. **81**, 3594 (1984).
[24] A. J. H. Wachters, J. Chem. Phys. **52**, 1033 (1970).
[25] C. E. Moore, *Atomic Energy Levels*, Natl. Bur. Stand. Circ. No. 467 (US GPO, Washington DC, 1949).
[26] (a) P. S. Bagus, K. Hermann, and C. W. Bauschlicher, J. Chem. Phys. **81**, 1966 (1984); (b) **80**, 4378 (1984).
[27] P. S. Bagus and F. Illas, J. Chem. Phys. **96**, 8962 (1992).
[28] J. P. Muscat and I. P. Batra, Phys. Rev. B **34**, 2889 (1986), and references therein.
[29] L. G. M. Pettersson and P. S. Bagus, Phys. Rev. Lett. **56**, 500 (1986).
[30] G. Pacchioni and P. S. Bagus, Surf. Sci. **269/270**, 669 (1992).
[31] See the discussion in F. Illas and P. S. Bagus, J. Chem. Phys. **94**, 1236 (1991).
[32] P. O. Garland, Phys. Nor. **6**, 201 (1972).
[33] L. Langmuir and K. H. Kingdon, Phys. Rev. **21**, 381 (1923).